# EFFECT OF VARIABLE THERMAL CONDUCTIVITY ON THE MHD BOUNDARY LAYER OF CASSON-NANOFLUID OVER A MOVING PLATE WITH VARIABLE THICKNESS

Hassan. N. ISMAIL[*], M. S. ABDEL-WAHED[*,1] and M. OMAMA[*,2]

* Basic Engineering sciences department, Faculty of Engineering at Benha, Benha University, Cairo, Egypt.
[1]E-mail: eng_moh_sayed@live.com [2]E-mail: mohamedomama@yahoo.com

*The effect of variable thermal conductivity on the characteristics of heat transfer and mechanical properties of a moving surface on a casson-nanofluid flow as a coolant has been studied in this paper. We used similarity transformation method to transform the equations of the governing boundary layer into ordinary differential equations which are solved numerically using a mix of fourth order Runge Kutta method and find root technique. Different values relevant parameters have been studied on the features of velocity, temperature and the profiles of concentration and discussed in details for different values of various parameter as shape parameter, heat source parameter, radiation parameter and magnetic parameter. The results were compared with previous published researches and obtained it in a good agreement and the results were tabulated. Furthermore, Nusselt number, Sherwood number and the Skin friction values with different parameters were calculated and the influence of theses physical quantities on the mechanical properties on the surface are analyzed and discussed in details.*

Keywords: casson fluid, Nanofluid, thermal conductivity, variable thickness, thermal radiation

## 1. Introduction

Nanotechnology is one of the main technologies of atomic and molecular engineering that has the potential to bring about changes in many science and engineering applications beyond the traditional technologies available, Nanotechnology has several branches and Nanofluid is considered one of the most important of these branches. Nanofluid can be exploited in vehicle thermal management, fuel cells, microelectronics, hybrid powered engines, pharmaceutical processes, engine cooling, heat exchanger and nuclear reactor coolant as noted by Sheikholeslami in his book [1]. It is known that conventional fluids for the heat transfer process are poor in the heat transfer like water, Oil and ethylene glycol. Nanofluid is an advanced technology that uses a mixture of the base fluid such as water or oil and nanoparticles such as silver (Ag), Copper oxide (CuO) and aluminum oxide ($Al_2O_3$) which improve the heat transfer process. Bashok [2] studied the nanofluids boundary layer of the flow around a movable surface. Gbadeyan [3] investigated the boundary layer of nanofluids flow with a boundary condition convective over a stretching sheet. The increase in nanoparticles has been found to increases the thermal conductivity, thus significantly improving heat transfer properties of nanofluid indicated by Olanrewaju et al [4]. Abdel-wahed et al. [5] studied the effect of Brownian motion on heat transfer of nanofluid flow on a moving surface with variable thickness and non-linear velocity. The effect of joule heating and hall current on rotating ferro-nanofluid on stretching plate is presented by Abdel-Wahed [6]. The effect of Lorentz force on blood flow in a vertical conduit has been studied by Abdel-wahed [7]. The weak concentration micropolar nanofluid flow and its heat transfer on steady/unsteady-moving surface presented by Abdel‑wahed [8].

When the difference between the surface and the ambient temperature is large the effect of radiation will become necessary. Hady et al. [9] investigated the effect of thermal radiation on the flow and heat transfer of nanofluid over a dynamic stretching sheet with nonlinear velocity in the thermal radiation presence. Madaki et al [10] presented flow and heat transfer of nanofluid over a stretching sheet with nonlinear velocity in the thermal radiation presence. Olanrewaju et al. [11] studied the

nanofluids flow boundary layer on a moving surface in the attendance of radiation. Abdel-Wahed et al. [12] investigated the heat transfer and the flow of nanofluids with a nonlinear velocity on a movable surface has a variable thickness in the radiation presence.

Magnetohydrodynamic (MHD) boundary layers flow of mass and heat transfer has a large effect for many engineering applications such as the thermal insulation and enhanced cooling of nuclear reactors. Magnetic field applications of circulatory system in the human artery and its applications were presented by Sharma et al. [13]. Hamad et al. [14] studied the magnetic field effects of nanofluid flow with free convection over a semi-infinite vertical flat plate. Abdel-wahed et al. [15] studied the boundary layer behavior of MHD nanofluid over a moving surface under the influence of convective boundary conditions. Khan et al. [16] investigated the nanofluid boundary layer of unsteady free convection flow on a stretching sheet with a magnetic field in the thermal radiation presence. An exact solution for the boundary layer of nanofluid flow over a movable surface with magnetic field presence has been obtained by Elbashbeshy et al. [17]. Recently, the magnetic field and nonlinear Rosseland thermal radiation effects on a flow and heat transfer of nanofluid around a moving surface with variable thickness studied by Abdel-wahed et al. [18]. Reddy et al. [19] deduced MHD Williamson nanofluid flow and heat transfer characteristics on a stretching sheet has a variable thickness and with thermal conductivity. Mohammadein et al. [20] presented the KKL-model of CuO-nanofluid MHD flow over a stagnation point stretching sheet in the presence of nonlinear thermal radiation and suction/injection. The effect of nonlinear thermal radiative and hall current on the flow of MHD Ferro-Nano fluid in a curved semi-porous tube has been studied by Abdel-wahed [21].
Casson fluid is another kind of non-Newtonian fluid because its characteristics have to do with shear stress and strain. A Casson fluid can described as a shear thinning liquid with infinite viscosity at zero shear rates, and zero viscosity at an infinite rate of shear, it works as a solid if the shear stress is less than yield stress applied to the fluid, while the move begins if the applied yield stress is less than shear stress. There are some examples of Casson Fluid like soup, jelly, honey, tomato sauce, concentrated fruit juices and Human blood. Hayat et al. [22] investigated MHD Casson fluid boundary layer of a flow of over a stretched sheet. Bhattacharyya et al. [23] deduced an analytical solution of a MHD Casson fluid flow past a permeable stretching sheet. Thiagarajan et al. [24] studied similarity solutions of a MHD Casson fluid flow past a shrinking sheet. Recently, Pushpalatha et al. [25] presented numerically unsteady Casson fluid flow around a stretching surface with thermal radiation and cross diffusion. The effect magnetic field and thermal radiation of a Casson nanofluid on a continuous surface has been studied by Ismail et al. [26].In this work, we will study the boundary layer of a Magnetohydrodynamic (MHD) casson nanofluid flow affected by variable thermal conductivity on a movable surface has a variable thickness and the effects of embedded parameters on the physical properties of the boundary layer and on the mechanical properties of the surface.

## 2. Problem formulation

Assume a viscous and incompressible casson nanofluid in two dimensional steady flow with a variable thermal conductivity $k$ around a movable surface has a variable thickness which has been identified as $y = \delta(x+b)^{\frac{1-n}{2}}$, furthermore, the surface is thin enough because the $\delta$ coefficient considered small and the plate is moving with nonlinear velocity $U_{w(x)} = a(x+b)^n$. The boundary layer is affected by nonlinear heat generation Q($x$), thermal radiation with heat flux $q_r$ and nonlinear transverse magnetic field $B(x)$, The fluid is supposed to be slightly connected, so that the Reynolds magnetic number is much lower than the unit and therefore the induced magnetic field is negligible compared to the applied magnetics. Assuming that fluid phase and nanoparticles are in a state of thermal equilibrium and that no slip happens between them.

Fig. 1 shows that the x-axis is along the plate in the direction of the surface movement and y- axis perpendicular to it. The boundary layer governing equations which describing the two-dimensional steady flow of MHD casson nanofluid on a moving surface with nonlinear Rosseland thermal radiation effect are written as the following [6] & [27] :-

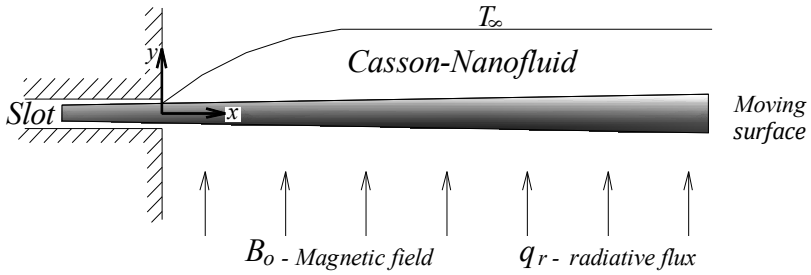


Fig.1. Physical model and coordinate system

$$\frac{\partial u}{\partial x}+\frac{\partial v}{\partial y}=0 \tag{1}$$

$$u\frac{\partial u}{\partial x}+v\frac{\partial u}{\partial y}=\mathcal{V}\frac{\partial^2 u}{\partial y^2}+\frac{1}{\beta}\frac{\partial^2 u}{\partial y^2}-\frac{\sigma B^2(x)}{\rho}u \tag{2}$$

$$u\frac{\partial T}{\partial x}+v\frac{\partial T}{\partial y}=\frac{1}{\rho C_P}\frac{\partial}{\partial y}\left(k\frac{\partial T}{\partial y}\right)-\frac{1}{\rho C_P}\frac{\partial q_r}{\partial y}+\tau\left[D_B\frac{\partial C}{\partial y}\frac{\partial T}{\partial y}+\frac{D_T}{T_\infty}\left(\frac{\partial T}{\partial y}\right)^2\right]+\frac{Q(x)}{\rho C_P}(T-T_\infty) \tag{3}$$

$$u\frac{\partial C}{\partial x}+v\frac{\partial C}{\partial y}=D_B\frac{\partial^2 C}{\partial y^2}+\frac{D_T}{T_\infty}\left(\frac{\partial^2 T}{\partial y^2}\right) \tag{4}$$

Where $u$ is the component of velocity in the $x$ direction and $v$ is the component of velocity in the $y$ direction, While $\mathcal{V},\beta,\sigma,\rho,\alpha,C_P,\tau,D_T,D_B$ are the kinematic viscosity, Casson fluid parameter, electrical conductivity, the base fluid density, thermal diffusion, the fluid heat capacity at constant pressure, the ratio between the nanoparticle effective heat capacity and the fluid heat capacity, Thermo-diffusion coefficient and Brownian diffusion coefficient.

The form of magnetic field strength $B(x)=B_0(x+b)^{\frac{n-1}{2}}$ and heat generation $Q(x)=Q_0(x+b)^{n-1}$ are assumed to get a similarity solution. Moreover, the thermal conductivity $k$ is assumed temperature dependent in the following form $k=k_\infty\left[1+\varepsilon\frac{T-T_\infty}{T_w-T_\infty}\right]$, Where $\varepsilon$ is Thermal conductivity parameter

The fluid is considered to absorb radiation; by using Rosseland approximation Clouet [28] defined the relative heat flux in the energy equation in the following form:

$$q_r=-\frac{4\sigma^*}{3\alpha^*}\frac{\partial T^4}{\partial y} \tag{5}$$

Where $\alpha^*$ and $\sigma^*$ are the mean absorption coefficient and the stefen-Boltzman constant respectively, $T^4$ can define as a temperature linear function, using Taylor series about $T_\infty$ for expending $T^4$ We get

$$T^4\cong 4TT_\infty^3-3T_\infty^4 \tag{6}$$

Using equations (5) and (6) in the equation of energy (3), we will get

$$u\frac{\partial T}{\partial x}+v\frac{\partial T}{\partial y}=\alpha\frac{\partial^2 T}{\partial y^2}+\frac{16\sigma T_\infty^3}{3\alpha(\rho C_P)}\frac{\partial^2 T}{\partial y^2}+\tau\left[D_B\frac{\partial C}{\partial y}\frac{\partial T}{\partial y}+\frac{D_T}{T_\infty}\left(\frac{\partial T}{\partial y}\right)^2\right]+\frac{Q(x)}{\rho C_P}(T-T_\infty) \tag{7}$$

Using boundary conditions

$$v = 0, \quad u = U_w, \quad T = T_w, \quad C = C_w \quad at\ y = \delta(x+b)^{\frac{1-n}{2}} \tag{8}$$

$$v = 0, \quad u = 0, \quad T = T_\infty, \quad C = C_\infty \quad at\ y \to \infty$$

The velocity, temperature and nanoparticle concentration are assumed as

$$U_{w(x)} = a(x+b)^n, \quad \theta(\eta) = \frac{T-T_\infty}{T_w-T_\infty}, \quad \phi(\eta) = \frac{C-C_\infty}{C_w-C_\infty} \tag{9}$$

Where *a and b* are constants, $T_w$ is the temperature of the surface, $T_\infty$ is the ambient temperature and $n$ is the shape parameter and it assumed that $n > -1$

**3. Similarity transformation**

In this section, We will apply a similarity solution to transform the equations (1),(2),(4) and (7) whose subjected to the boundary conditions (8) to an ordinary differential equations system using the following dimensionless functions:

$$\varphi = \sqrt{\left(\frac{2}{(n+1)}\right)(x+b)^{n+1}a\mathcal{V}}\,\mathrm{F}(\eta), \qquad \eta = y\sqrt{\left(\frac{n+1}{2}\right)\left(\frac{a(x+b)^{n-1}}{\mathcal{V}}\right)} \tag{10}$$

Where $\varphi$ is the stream function where $u = \frac{\partial\varphi}{\partial y}$, $v = -\frac{\partial\varphi}{\partial x}$ and $\eta$ is the similarity variable

Substituting (8) into (2) and (6) get the following ordinary differential equations

$$(1+\frac{1}{\beta})F''' + FF'' - \left(\frac{2n}{n+1}\right)F'^2 - \left(\frac{2M}{n+1}\right)MF' = 0 \tag{11}$$

$$\left(\frac{4Rd+3}{3P_r}\right)((1+\varepsilon\theta)\theta'' + \varepsilon\theta'^2) + F\theta' + Nb\phi'\theta' + Nt\theta'^2 + \left(\frac{2\lambda}{n+1}\right)\theta = 0 \tag{12}$$

$$\phi'' + \frac{1}{2}LeF\phi' + \left(\frac{Nt}{Nb}\right)\theta'' = 0 \tag{13}$$

With boundary conditions

$$\theta(0) = 1, \theta(\infty) = 0, F(\alpha) = \alpha\left(\frac{1-n}{1+n}\right), F'(\alpha) = 1, F'(\infty) = 0, \phi(0) = 1\ and\ \phi(\infty) = 0 \tag{14}$$

Note that the differentiation here is related to $\eta$. By defining $F(\eta) = f(\eta - \alpha) = f(\zeta)$, the similarity equations (11)-(13) and the associated boundary conditions (14) become

$$(1+\tfrac{1}{\beta})f''' + ff'' - \left(\tfrac{2n}{n+1}\right)f'^2 - \left(\tfrac{2M}{n+1}\right)Mf' = 0 \tag{15}$$

$$\left(\frac{4Rd+3}{3P_r}\right)((1+\varepsilon\theta)\theta'' + \varepsilon\theta'^2) + f\theta' + Nb\phi'\theta' + Nt\theta'^2 + \left(\frac{2\lambda}{n+1}\right)\theta = 0 \tag{16}$$

$$\phi'' + \frac{1}{2}LeF\phi' + \left(\frac{Nt}{Nb}\right)\theta'' = 0 \tag{17}$$

With boundary conditions

$$f(0)=\alpha\left(\frac{1-n}{1+n}\right), f'(0)=1, \theta(0)=1, \phi(0)=1 \quad and \quad f'(\infty)=0, \theta(\infty)=0, \phi(\infty)=0 \qquad (18)$$

Where

$$\beta=\frac{\mu_B\sqrt{2\pi_c}}{P_y}, M=\frac{\sigma B_0^2}{\rho a}, \mathrm{Rd}=\frac{4\sigma T_\infty^3}{\alpha K_f}, P_r=\frac{\nu}{\alpha}, Nb=\frac{\tau D_B}{\nu}(C_w-C_\infty), Nt=\frac{\tau D_T}{\nu T_\infty}(T_w-T_\infty), Le=\frac{\nu}{D_B},$$

$$\lambda=\frac{Q_0}{a\rho C_P} \text{ And } \tau=\frac{(\rho C_P)_p}{(\rho C_P)_f} \qquad (19)$$

Where M is magnetic field parameter, $P_r$ is prandtl number, $Nb$ is the Brownian motion parameter, $Nt$ is the thermophoresis parameter, $Le$ is the lewis number and $\lambda$ is the heat source parameter.

**4- Method of Solution**

The equations (15)-(17) are solved numerically with boundary conditions (18). First, to be able to solve this system, the unknown initial conditions $f''(0), \theta'(0)$ and $\phi'(0)$ should be computed so a program for this system is created as an initial value problem with the missing of the initial conditions. For solving this system, we must suggest a suitable value of $\eta \longrightarrow \infty$ $''\eta_\infty''$, and then, the missing values are calculated by the code using find root technique. When the values $f''(0), \theta'(0)$ and $\phi'(0)$ do not change with the increase of $\eta \longrightarrow \infty$ (i.e. boundary conditions $f'(\eta_\infty)=0$, $\theta'(\eta_\infty)=0$ $and$ $\phi'(\eta_\infty)=0$ satisfied at the suggested value of $(\eta \longrightarrow \infty)$, becomes ready for solving the system using the fourth order Explicit Runge–Kutta method with step size $\Delta\eta = 0.01$. To confirm the results gained from this method, (Table 1) and (Table 2) were used to compare the results for $\theta'(0)$ and $\phi'(0)$ with the numerical solution gained in this study and the numerical solution obtained by Madaki et al. [10].

**Table 1. $-\theta'(0)$ And $-\phi'(0)$ values for Rd = $n = \alpha$ =M= 0.3, $\beta = \infty$, Le =2, Pr = 6.2, $Nb$ = 0.1, Pr = 6.2, $\varepsilon = 0$ , Nt = 0.1 and various value of $\lambda$**

| $\lambda$ | Madaki et al. [10] | | current results | |
|---|---|---|---|---|
| | $-\theta'(0)$ | $-\phi'(0)$ | $-\theta'(0)$ | $-\phi'(0)$ |
| **-0.3** | 1.3092 | 0.4001 | 1.3094 | 0.4000 |
| **-0.1** | 1.0631 | 0.1737 | 1.0631 | 0.1737 |
| **0** | 0.9128 | 0.0371 | 0.9128 | 0.0370 |
| **0.1** | 0.7284 | 0.1287 | 0.7285 | 0.1289 |
| **0.3** | 0.1397 | 0.8901 | 0.1397 | 0.8900 |

**Table 2. $-\theta'(0)$ and $-\phi'(0)$ values for Rd = 1, $\alpha = n$ = M = 0.6, $\beta = \infty$, Le =2, $Nb$ = 0.1, Pr = 6.2, $\lambda = 0.2$, $\varepsilon = 0$ and various value of Nt**

| $Nt$ | Madaki et al.[10] | | current results | |
|---|---|---|---|---|
| | $-\theta'(0)$ | $-\phi'(0)$ | $-\theta'(0)$ | $-\phi'(0)$ |
| **0.1** | 0.0349 | 0.7331 | 0.0348 | 0.7331 |
| **0.4** | 0.1106 | 1.3319 | 0.1105 | 1.3318 |
| **0.6** | 0.1761 | 2.0651 | 0.1760 | 2.0650 |

## 5. Results

The most important characteristic of flows are Nusselt number, skin friction and Sherwood number coefficient, which physically correspond with the rate of heat transfer, the surface shear stress, and the rate of mass transfer respectively. These characteristics have a direct effect during the cooling process on the surface mechanical properties, such as if the heat transfer rate of the surface increased the surface cooling will accelerates, causing an improvement of the shear strength and hardness of the surface, but increases surface cracking and decrease its ductility.

### 5.1 Surface shear stress

$$\tau_w = \left(1+\frac{1}{\beta}\right)\mu\left(\frac{\partial u}{\partial y}\right)_{y=\delta(x+b)^{\frac{1-n}{2}}} = \left(1+\frac{1}{\beta}\right)\mu\sqrt{\frac{a^3}{v}\left(\frac{n+1}{2}\right)(x+b)^{3n-1}}f''(0) \qquad (20)$$

The coefficient of skin friction is given by $C_{fx} = \frac{2\tau_w}{\rho U_w^2}$ (21)

Then, the skin friction $\sqrt{Re}C_{fx} = 2\left(1+\frac{1}{\beta}\right)\sqrt{\frac{n+1}{2}}f''(0)$ (22)

### 5.2 Surface heat flux

$$q_w = (q_r)_w - K\left(\frac{\partial T}{\partial y}\right)_{y=\delta(x+b)^{\frac{1-n}{2}}} = -K(T_w - T_\infty)\sqrt{\frac{a}{v}\left(\frac{n+1}{2}\right)(x+b)^{n-1}}\left(\frac{4Rd}{3}+1\right)\theta'(0) \qquad (23)$$

The Nusselt number (Nu) is given by $\frac{(X+b)\,q_w}{K(T_w - T_\infty)}$ (24)

Then, Nusselt number $\frac{Nu}{\sqrt{\mathrm{Re}}} = -(\frac{4Rd}{3}+1)\sqrt{\frac{n+1}{2}}\ \theta'(0)$ (25)

### 5.3 Surface mass flux

$$q_m = -D_B\left(\frac{\partial c}{\partial y}\right)_{y=\delta(x+b)^{\frac{1-n}{2}}} = -D_B(C_w - C_\infty)\sqrt{\frac{a}{v}\left(\frac{n+1}{2}\right)(x+b)^{n-1}}\ \phi'(0) \qquad (26)$$

The Sherwood number (Sh) is given by $\frac{(X+b)\,q_m}{D_B(C_w - C_\infty)}$ (27)

Then, Sherwood number $\frac{Sh}{\sqrt{\mathrm{Re}}} = -\sqrt{\frac{n+1}{2}}\ \phi'(0)$ (28)

Where $\mathrm{Re} = \frac{u_w(x+b)}{v}$

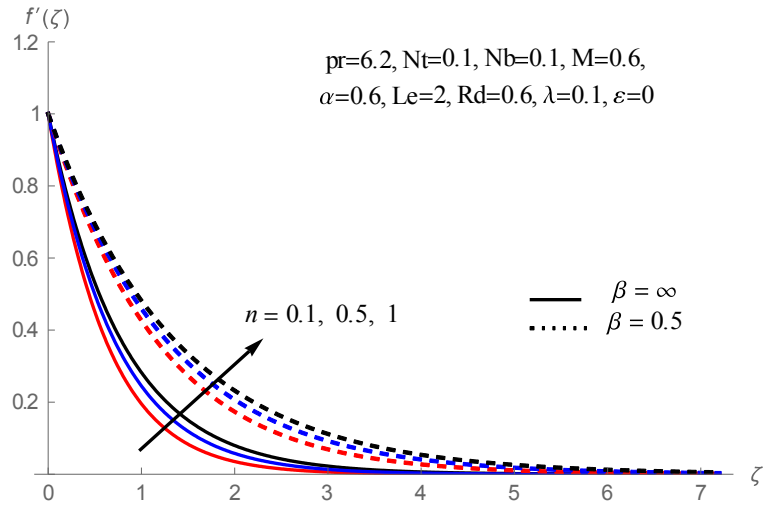


Fig. 2. Velocity profiles of the different values of $n$ and $\beta$

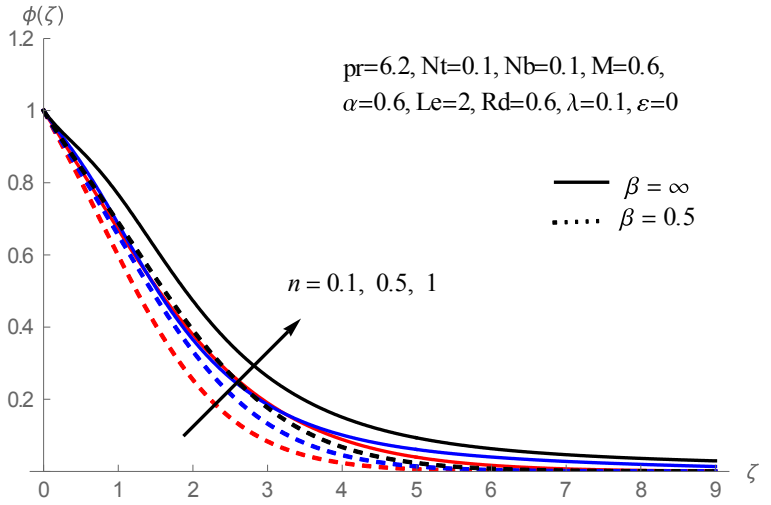


Fig. 3. Concentration profiles of the different values of $n$ and $\beta$

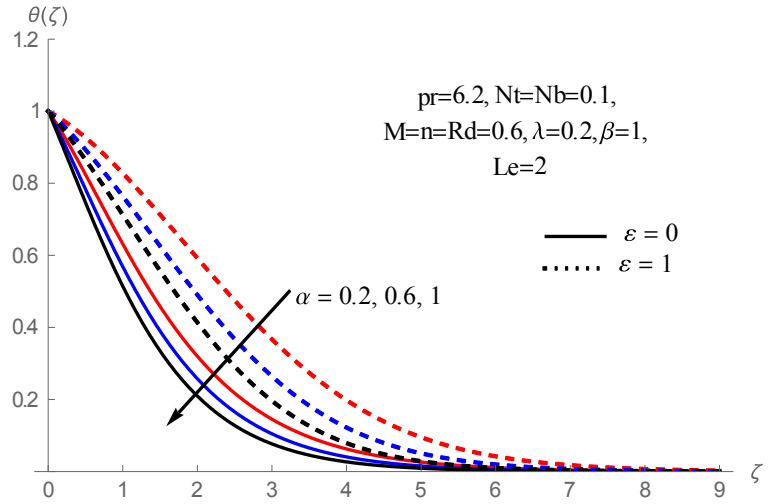


Fig. 4. Temperature profiles of the different values of α and ε

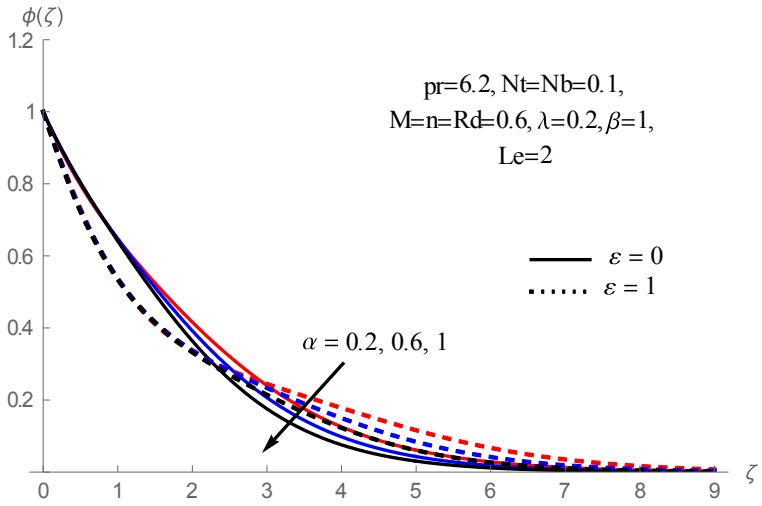


Fig. 5. Concentration profiles of the different values of α and ε

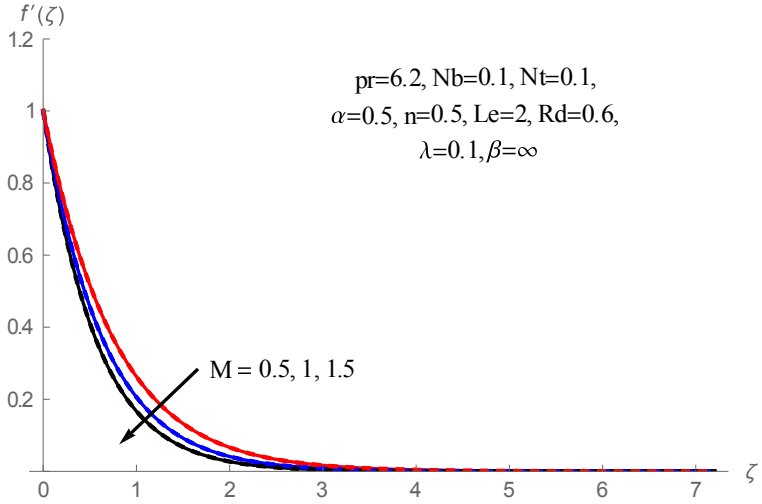


Fig. 6. Velocity profiles of the different values of M

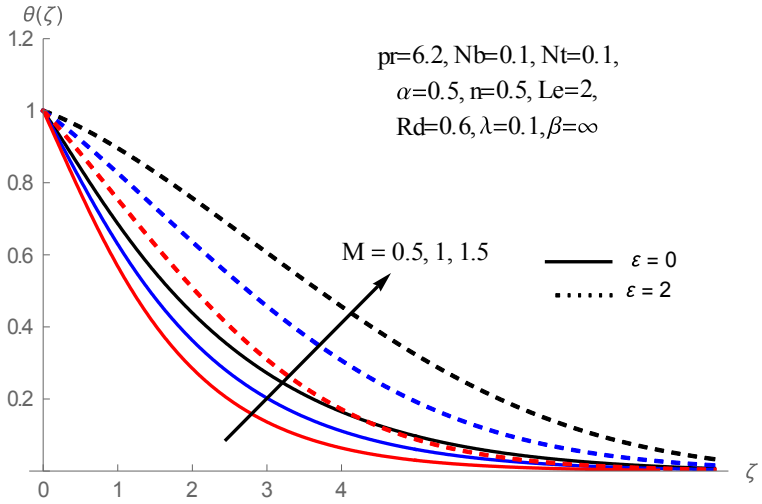


Fig. 7. Temperature profiles of the various values of M and ε

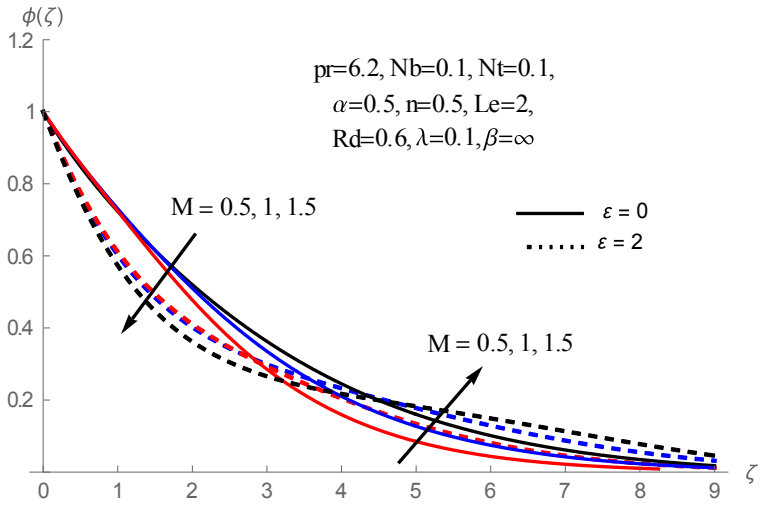


Fig. 8. Concentration profiles of the different values of M and ε

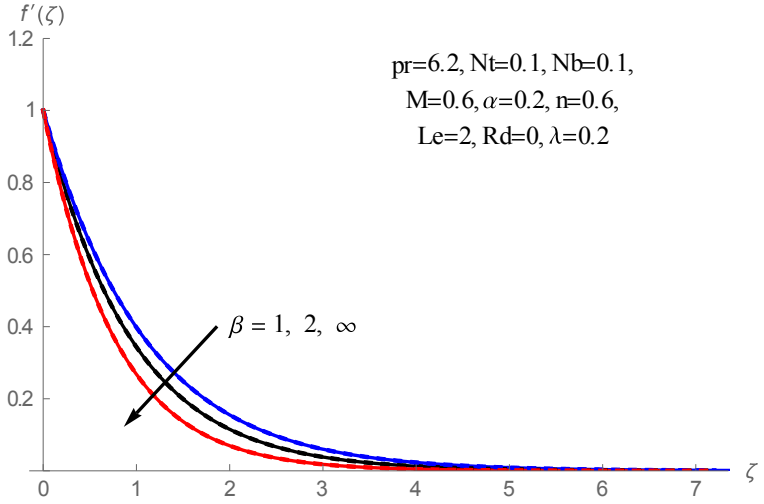


Fig. 9. Velocity profiles of the different values of Casson parameter $\beta$

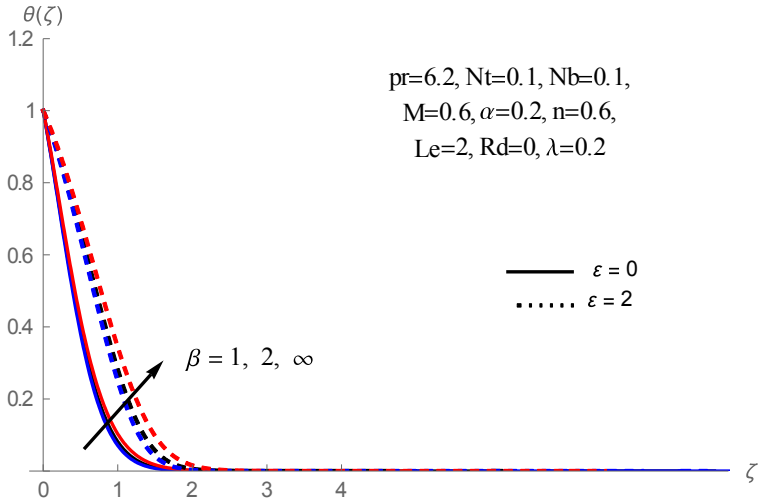


Fig. 10. Temperature profiles of the various values of Casson parameter $\beta$ and ε

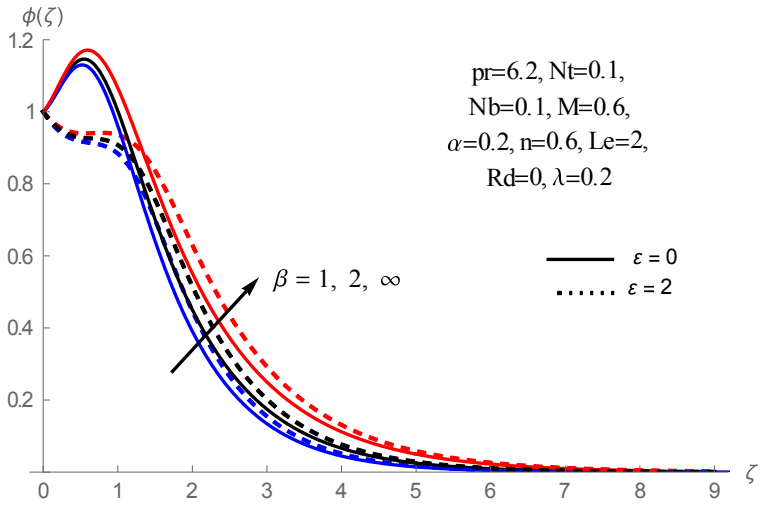


Fig. 11. Concentration profiles of the different values of Casson parameter $\beta$ and ε

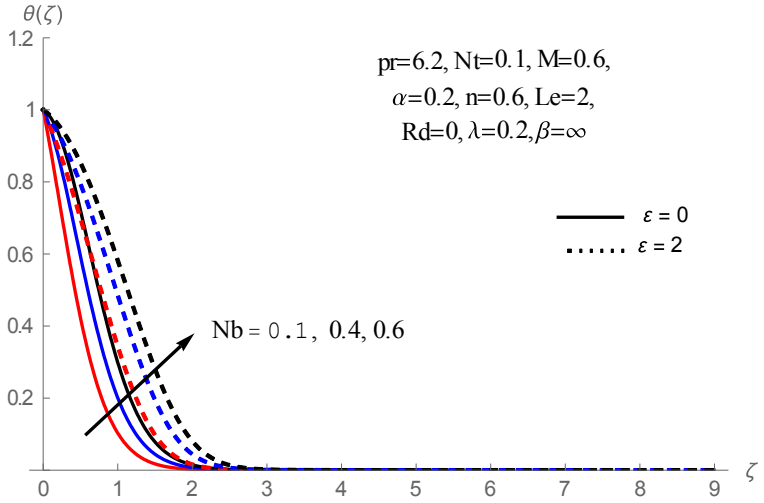


Fig. 12. Temperature profiles of the different values of Nb and ε

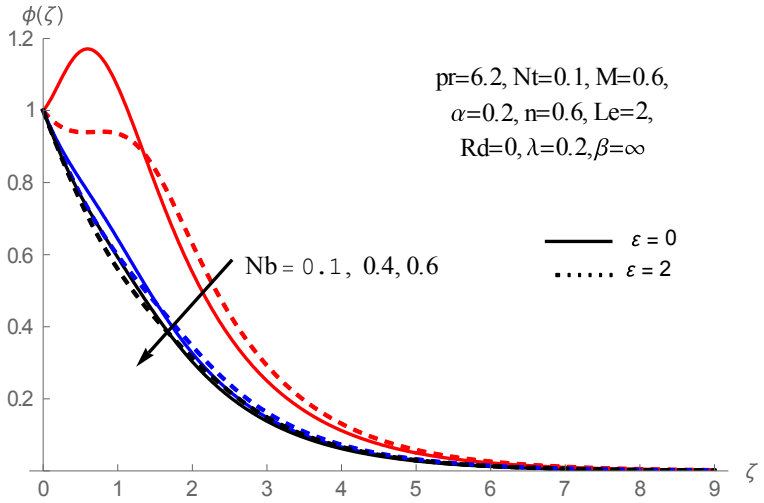


Fig. 13. Concentration profiles of the different values of Nb and ε

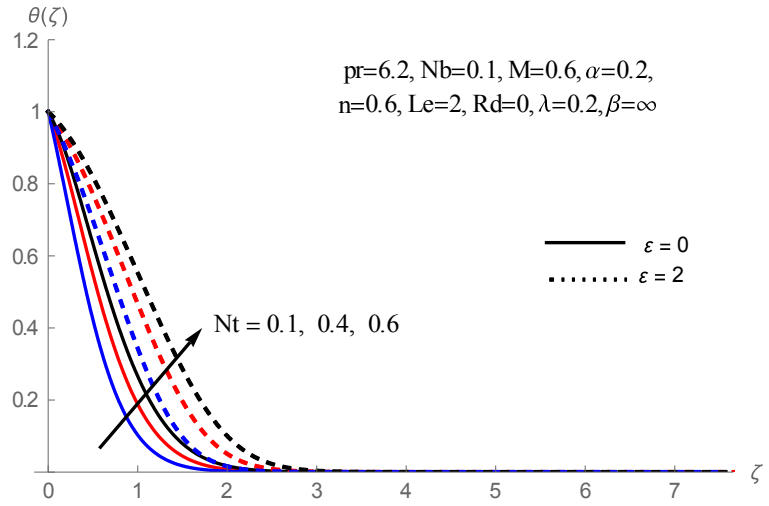


Fig. 14. Temperature profiles of the various values of Nt and ε

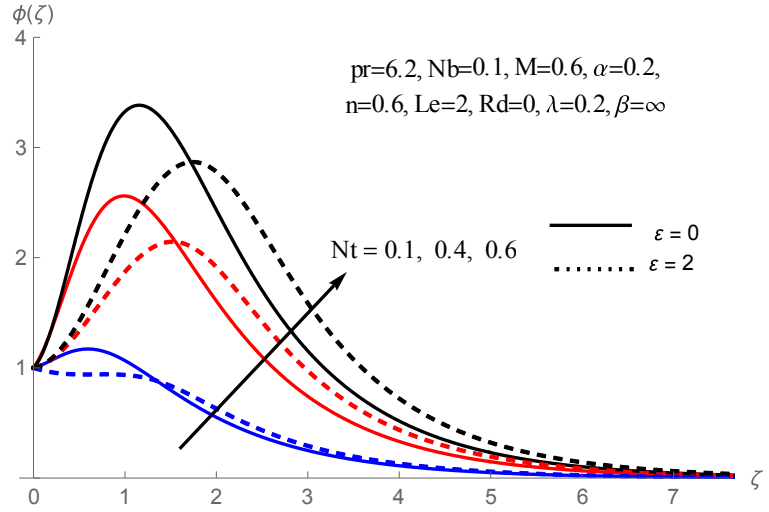


Fig. 15. Concentration profiles of the different values of Nt and ε

**Table 3. The effects of n and $\beta$ on $-f''(0)$, $-\theta'(0)$ and $-\phi'(0)$ along their associated $C_{fx}$, Nu and Sh number when $Rd = \alpha = M = 0.5$, Le =2, $Nb = Nt = 0.1$, $Pr = 6.2$, $\lambda = 0.2$ and $\varepsilon = 0$**

| $n$ | β | $-f''(0)$ | $-\theta'(0)$ | $-\phi'(0)$ | $C_{fx}\sqrt{Re}$ | $\frac{Nu}{\sqrt{Re}}$ | $\frac{Sh}{\sqrt{Re}}$ |
|---|---|---|---|---|---|---|---|
| **0.5** | ∞ | 1.2928 | 0.0875 | 0.6162 | -2.2391 | 0.1262 | 0.5336 |
| **1** | | 1.2247 | 0.1704 | 0.4480 | -2.4494 | 0.2840 | 0.4480 |
| **1.5** | | 1.1882 | 0.2067 | 0.3661 | -2.6568 | 0.3850 | 0.4093 |
| **0.5** | 2 | 1.0420 | 0.4003 | 0.4375 | -2.7070 | 0.5776 | 0.3788 |
| **1** | | 1.0000 | 0.3508 | 0.3820 | -3.0000 | 0.5846 | 0.3820 |
| **1.5** | | 0.9773 | 0.3305 | 0.3449 | -3.2779 | 0.6158 | 0.3846 |

**Table 4. The effects of n and ε on $-f''(0)$, $-\theta'(0)$ and $-\phi'(0)$ along their associated $C_{fx}$, Nu and Sh number when Rd =0, $\alpha = 0.5$, M = 0.6, Le =2, Nb = Nt = 0.1, Pr = 6.2, $\lambda = 0.2$ and $\beta = \infty$**

| $n$ | $\varepsilon$ | $-f''(0)$ | $-\theta'(0)$ | $-\phi'(0)$ | $C_{fx}\sqrt{Re}$ | $\frac{Nu}{\sqrt{Re}}$ | $\frac{Sh}{\sqrt{Re}}$ |
|---|---|---|---|---|---|---|---|
| **0.3** | 0 | 1.4009 | 1.9029 | -0.9361 | -2.2588 | 1.5341 | -0.7547 |
| | 0.1 | 1.4009 | 1.7537 | -0.7922 | -2.2588 | 1.4138 | -0.6386 |
| | 0.2 | 1.4009 | 1.6280 | -0.6717 | -2.2588 | 1.3125 | -0.5415 |
| **0.6** | 0 | 1.3252 | 1.3654 | -0.4966 | -2.3705 | 1.2212 | -0.4441 |
| | 0.1 | 1.3252 | 1.2686 | -0.4055 | -2.3705 | 1.1346 | -0.3626 |
| | 0.2 | 1.3252 | 1.1866 | -0.3287 | -2.3705 | 1.0613 | -0.2939 |

## 6. Discussion

It should be noted that the surface external shape is absolutely dependent on ($n$) values. The study was significantly reduced to a stable thickness of a flat surface when n = 1, whereas in n > 1 this analysis turns into a low thickness surface and a recessed external shape. Also when n <1 this analysis has been reconstituted in a surface with increasing thickness and an arched outer shape, Furthermore, from the casson nanofluid concept when Casson parameter ($\beta$) value is ∞ this means that the effect of casson nanofluid is vanish. And the fluid has become traditional nanofluid. Also, It should be noted that when the thermal conductivity parameter ($\varepsilon$) vanishes, the flow return to flow with constant thermal conductivity.

The influences of the governing parameters n, β, α, ε, M, Nb and Nt on the velocity, temperature and nanoparticles concentration are sketched in figures 2–15. Moreover, table 3 and 4 show the values of temperature, velocity and concentration gradient and corresponding values of the Nusselt number, the skin friction and the Sherwood number of various values of ($\beta$ *with* $n$) and (ε with $n$) respectively.

Figures (2) and (3) describe the effect of the shape parameter ($n$) on the concentration and velocity. It is found that both the concentration and the velocity increase with the increase in shape parameter. Also one can observe that, the velocity of the casson flow is greater than the regular nanofluid flow at the same conditions and the opposite occur for the concentration

Figures (4) and (5) represent the influence of the parameter of the thickness (α) on the temperature and concentration. It is found that, both the temperature and the concentration are decreases with increase in the thickness parameter, these figures clear in agreement with the physical behavior whenever the surface thickness decreases whenever the treatment process accelerates. As well in fig (4) and (5), the effect of variable thermal conductivity parameter ($\varepsilon$) with increase of thickness parameter studied, it has been found that the up-variation of the thermal conductivity will increase the temperature and the same behavior occur for the concentration but near the boundary layer end.

The influence of magnetic field parameter (M) on velocity, temperature and concentration profiles are showed in figures (6), (7) and (8). It has been found that the increase in the parameter of magnetic field will decrease the velocity, because the Lorentz force will increase when magnetic field parameter increases and this lead to oppose the motion of the fluid. But the temperature and concentration are increase due to the increasing of magnetic field parameter, and this effect is clearer near the surface and vanishing as we go far away from the surface.

On the other hand, when we take in mind the variation of the thermal conductivity (ε) with increase of M, one can found that the temperature increases for the increasing of the thermal conductivity parameter. Moreover, the concentration decreases until η<4 and then returns to increases for η>4

In figures (9), (10) and (11) the influence of the casson parameter (β) are shown. It is appeared that when casson parameter is increase the velocity decreases but concentration and temperature are increase. It is worth mentioning that increasing of the casson parameter leads to reduce the yield stress and when (β) continue to increase even ($\beta \to \infty$)the casson nanofluid behaves becomes like pure Newtonian nanofluid, it is means that the velocity of Casson nanofluid is greater than the velocity of pure Newtonian nanofluid, but the temperature and concentration of pure Newtonian nanofluid is greater. Furthermore, it is clear from these graphs that the up-variation in thermal conductivity will increase the concentration and the temperature. It is worth mentioning that for the constant thermal conductivity, the concentration of the particles increases to the maximum near the surface before decaying to zero and this maximum level transfer to flat level of concentration for the variable thermal conductivity

Due to the fast moving of throwing of molecules or atoms in fluid the motion of particles suspended in fluid will has a random movement which called by Brownian motion. This movement influences and controls the temperature and concentration of particles within the surface boundary layer. The parameter of Brownian motion (Nb) has very important effect in this study, In Figures (12) and (13) we found that when Nb is increase the temperature increases and decreases the nanoparticles concentration, and as we mentioned that the Brownian motion refers to particle movement, so, activation of the movement of particles increases the heat produced and will rise the temperature. Also in fig (12) and (13) When we study the effect of the variable thermal conductivity parameter ($\varepsilon$) with increase of Brownian motion parameter, we found that the temperature increases and concentration profile decreases
Another important phenomenon is the Thermophoresis phenomenon which may be observed in the moving particles mixtures, Because of the difference in particle types, the responses are different for the temperature gradient force. In this study this phenomenon effect is appears in the thermophoresis parameter (Nt) such that the increase in this parameter leads to increase of temperature and nanoparticle concentration of the boundary layer, apparently in Figs. (14) and (15), this is because the force of the thermophoresis was developed by the surface rate of mass transfer creates a far smooth flow from the nonlinear stretching surface, hence, with much quantities of thermophoresis the fluid is more heated shift away from the surface, and because of the thermophoresis force presence the flow is fast from the nonlinear surface and that's lead to increasing the nanoparticle concentration boundary layer. Also fig (14) and (15) show the effect of variable thermal conductivity parameter ($\varepsilon$) with the increase in (Nt), it leads to increase of the temperature and concentration profile decreases

table 3 show the values of the gradient of temperature, velocity and concentration on the surface with the thickness parameter varying for both the regular and casson nanofluids and according to the relations (22,25, and 28) the corresponding values of the skin friction, Nusselt number and Sherwood number are computed in this table.
Generally, one can observe that, the Nusselt number and the skin friction increase gradually by increasing of the parameter of shape ($n$) at any value of β, and Sherwood number decreases with increase of ($n$) parameter for regular nanofluids ($\beta = \infty$), otherwise, increases with increase of ($n$) parameter for the casson nanofluid ($\beta = 2$). It is worth mentioning that, the increasing of surface skin friction and the Nusselt number, meaning increase of shear stress on the surface and accelerating the cooling process due to high heat flux.

table 4 used to show the numerical gradient values of temperature, velocity and concentration on the surface with the variation of both the shape parameter ($n$) and the thermal conductivity parameter ($\varepsilon$) and corresponding values of the Nusselt number, the skin friction and the Sherwood number are

computed in this table. It is clear that, the raising of the thermal conductivity parameter ($\varepsilon$) and the shape parameter ($n$) leads to increase of the surface shear stress, and decrease the heat transfer rate and mass transfer rate.
Moreover, table 4 show that the increase of thermal conductivity parameter ($\varepsilon$) when (n) is constant have no effect on shear stress of the surface and skin friction, but decreases the Sherwood number and the Nusselt number which means decreasing the rate of mass transfer and the rate of heat transfer on the surface. That's because increasing in ($\varepsilon$) increases the thermal conductivity which reduce the heat gradually at the surface. It should be noted that decreasing heat transfer rate from the surface leads to a slow cooling process, which has a negative influence on the mechanical properties of the surface, such as stiffness, strength and hardness.

## 7. Conclusion

This research submit a mathematical model for a Magnetohydrodynamic casson nanofluid flow over a continuous surface moving with a variable thickness and variable thermal conductivity in the presence of thermal radiation and heat generation. Boundary layer behavior under the proposed forces and their effect on the mass transfer and heat transfer characteristics and the surface mechanical properties were the aim from this study and we obtained the following conclusions:

- Presence of Brownian motion and the Thermophoresis phenomena are very useful for increasing the heat transfer rate and accelerating the cooling process.
- Brownian motion decreases the rate of mass transfer at the surface. On the other side, Thermophoresis phenomena increase the rate of mass transfer at the surface.
- Raising the shape parameter ($n$) in both nanofluid and casson nanofluid increases the shear stress and the rate of heat transfer at the surface.
- The rate of mass transfer increases when ($n$) increase in nanofluid and decreases in case of using casson nanofluid
- Whenever thickness parameter (α) decreases, would have been better, this is because the lower the thickness of the surface gradually accelerates the cooling process
- Using casson nanofluid will increase the heat transfer rate over the surface which will accelerate the cooling process and this in turn leads to improve the heat treatment process, Also casson nanofluid increasing the shear stress on the surface and the rate of mass transfer over the surface.
- Raising the thermal conductivity ($\varepsilon$) decreases the rate of heat and mass transfer over the surface, but has no effect on shear stress on the surface and skin friction. Which adversely effect on the surface mechanical properties, such as stiffness and strength.

## Acknowledgement

This study has no fund and the author declare that he has no conflict of interest

## References


[1] M. Sheikholeslami, Application of Nanofluid for Heat Transfer Enhancement, EEE-5425, (2013).

[2] N. Bachok, A. Ishak, and I. Pop, Boundary-layer flow of nanofluids over a moving surface in a flowing fluid, *International Journal of Thermal Sciences vol. 49*, (2010) pp. 1663-1668.

[3] J. A. Gbadeyan, M. A. Olanrewaju, and P. O. Olanrewaju, Boundary Layer flow of a nanofluid past a Stretching sheet, *Australian Journal of Basic and Applied Sciences vol. 5(9),* (2011), pp. 1323-1334.

[4] P. O. Olanrewaju, O. T. Arulogun, and K. Adebimpe, Internal Heat Generation Effect on Thermal Boundary layer, *American Journal of Fluid Dynamics, vol. 2(1),* (2012), pp. 1-4.

[5] M.S. Abdel-wahed, E.M.A. Elbashbeshy and T.G. Emam, Flow and heat transfer over a moving surface with non-linear velocity and variable thickness in a nanofluid in the presence of Brownian motion, *Applied Mathematics and Computation, vol. 254*, (2015), pp. 49-62.

[6] M. S. Abdel-Wahed, Rotating ferro-nanofluid over stretching plate under the effect of hall current and joule heating, *Journal of Magnetism and Magnetic Materials, vol. 429*, (2017), pp. 287-293.

[7] M. S. Abdel-Wahed, Lorentz force effect on mixed convection micropolar flow in a vertical conduit, The European Physical Journal Plus, vol. 132(5), (2017), pp. 195,

[8] M. S. Abdel-wahed, Flow and heat transfer of a weak concentration micropolar nanofluid over steady/unsteady-moving surface*, applied Physics A, vol. 123(3)*, (2017), pp. 1-10, DOI 10.1007/s00339-017-0815-7

[9] F. M. Hady, F. S. Ibrahim, S. M. Abdel-Gaied, and M. R. Eid, Radiation effect on viscous flow of a nanofluid*, Nanoscale Research Letters, vol. 7*, (2012), pp. 229.

[10] A. G. Madaki, R. Roslan and I. Hashim, Flow and Heat Transfer of Nanofluid over a Stretching Sheet with Non-linear Velocity in the Presence of Thermal Radiation and Chemical Reaction, *Journal of Engineering and Applied Sciences, vol. 1830*, (2017), pp. 1-10.

[11] P. Olanrewaju, O. T. Arulogun, and K. Adebimpe, Internal Heat Generation Effect on Thermal Boundary layer, *American Journal of Fluid Dynamics, vol. 2*, (2012), pp. 1-4.

[12] E. M. A. Elbashbeshy, T. G. Emam, and M. S. Abdel-Wahed, Flow and heat transfer over a moving surface with nonlinear velocity and variable thickness in a nanofluid in the presence of thermal radiation, *Can. J. Phys. vol. 92*, (2013), pp. 124-130.

[13] M. K. Sharma, K. Singh and S. Bansal, Effect of Branch Angle and Magnetic Field on the Flow through a Bifurcating Vessel, *Journal of Mathematics, vol. 11*, (2015), pp. 8-20, , DOI: 10.9790/5728-11250820.

[14] M. A. A. Hamad, I. Pop, and A. I. M. Ismail, Magnetic field effects on free convection flow of a nanofluid, *Nonlinear Analysis: Real World Applications, vol. 12*, (2011), pp. 1338-1346.

[15] M. S. Abdel-wahed and T. Emam, MHD Boundary Layer Behaviour over a Moving Surface in a Nanofluid under the Influence of Convective Boundary Conditions, *Journal of Mechanical Engineering, vol. 63,* , (2017), pp. 119-128.

[16] W. A. Khan and I. Pop, Free convection boundary layer flow past a horizontal flat plate, *International Journal of Thermal Sciences, vol. 56*, (2012), pp. 48-57.

[17] E. M. A. Elbashbeshy, T. G. Emam, and M. S. Abdel-Wahed, An exact solution of boundary layer flow over a moving surface, *Heat Mass Transfer vol. 50*, (2013), pp. 57-64,

[18] M. S. Abdel-wahed, Nonlinear Rosseland thermal radiation and magnetic field effects on flow and heat transfer over a moving surface with variable thickness in a nanofluid, *Canadian Journal of Physics, vol. 95*, (2017), pp. 267-273.

[19] S. Reddy, K. Naikoti and M. M. Rashidi, MHD flow and heat transfer characteristics of Williamson nanofluid over a stretching sheet with variable thickness and variable thermal

conductivity, *Transactions of A. Razmadze Mathematical Institute, vol. 171*, (2017), pp. 195-211,
[20] S.A. Mohammadein, K. Raslan and M.S. Abdel-Wahed, KKL-model of MHD CuO-nanofluid flow over a stagnation point stretching sheet with nonlinear thermal radiation and suction/injection, *Results in Physics, vol. 10*, (2018) , pp. 194-199.
[21] M. S. Abdel-wahed, Magnetohydrodynamic Ferro-Nano fluid flow in a semi-porous curved tube under the effect of hall current and nonlinear thermal radiative, *Journal of Magnetism and Magnetic Materials, vol. 474*, (2019), pp. 347-354
[22] T. Hayat, S. A. Shehzad, and A. Alsaedi, Soret and Dufour effects on (MHD) flow of Casson fluid, *Applied Mathematics and Mechanics, vol. 33*, (2012), pp. 1301-1312, DOI: 10.1007/s10483-012-1623-6.
[23] K. Bhattacharyya, T. Hayat, and Ahmed Alsaedi, Analytic solution for Magnetohydrodynamic boundary layer flow of Casson fluid, Chinese Physics Journal, vol. 22, (2013), pp. 1-6, DOI: 10.1088/1674-1056/22/2/024702.
[24] K. Senthilkumar and M. Thiagarajan, DTM-Pade Approximants of MHD Boundary-Layer Flow of a Casson Fluid, *United States of America Research Journal, vol. 1*, (2013), pp. 1,
[25] K. Pushpalatha, Numerical study of chemically reacting unsteady Casson fluid flow, *Open Eng, vol. 7*, (2017), pp. 69-76.
[26] Hassan. N. Ismail, Adel A. Megahed, M. S. Abdel-Wahed, and M. Omama, Thermal Radiative Effects on MHD Casson Nanofluid Boundary Layer Over a Moving Surface, *Journal of Nanofluids, vol. 7,* (2018), pp. 910-916.
[27] J. D. Anderson, Governing Equations of Fluid Dynamics. *Computational Fluid Dynamics* (1992). DOI: https://doi.org/10.1007/978-3-662-11350-9_2.
[28] J. F. HYPERLINK , Clouet, The Rosseland approximation for radiative transfer problems in heterogeneous media, *Journal of Quantitative Spectroscopy and Radiative Transfer, vol. 58*, , (1997), pp. 33-43